SIMULATION OF AN INPUT SHAPING SCHEME TECHNIQUE TO INVESTIGATE UNWANTED NOISE AND VIBRATION IN WIPER BLADE

M.A.Salim[1], M. Z. Md Zain[2], A.R Abu-Bakar[3], A.Noordin[4]

[1]Faculty of Mechanical Engineering, Universiti Teknikal Malaysia Melaka, Locked Bag 1752, Durian Tunggal Pos Office, 76109, Durian Tunggal, Melaka, Malaysia

[2,3]Faculty of Mechanical Engineering, Universiti Teknologi Malaysia, 81310 Skudai, Johor Bahru, Johor, Malaysia

[4]Faculty of Electrical Engineering, Universiti Teknikal Malaysia Melaka, Locked Bag 1752, Durian Tunggal Pos Office, 76109, Durian Tunggal, Melaka, Malaysia

[1]azli@utem.edu.my, [2]zarhamdy@fkm.utm.my, [3]arahim@fkm.utm.my,[4]aminurrashid@utem.edu.my

ABSTRACT

Wiper system in automobile has a potential to generate noises. These noises can be categories into three types namely squeal, chattering and reversal noise. The squeal noise or squeaky noise appears at frequency 1000 Hz, the chattering noise appears at frequency 100 Hz and lastly is the reversal noise appears at 500 Hz. These noises lead to poor visibility and annoying sound to the driver and passengers, respectively. This paper describes a control technique that it is capable to reduce the unwanted noise and vibration level in automobile windshield wiper system. In this research, the derivation of two dimensional mathematical model of wiper system is produced using Newtonian approach and MATLAB/Simulink is used to simulate and analyze the vibration response of the wiper system in time domain and frequency domain. In this simulation, an input shaping scheme has been introduced as the control strategy. The simulation result has been verified by comparing with the result obtained using numerical approach analysis. The result shows that input shaping technique can reduce the vibration level to 25 to 30 percents compare the model with conventional scheme.

KEYWORDS: Wiper system, input shaping scheme, analytical and numerical approach

1.0 INTRODUCTION

Recently, the industry of automotive has been growing all over the world. Two components are required to be considered in order to make sure that automobile industry running in smooth conditions. The first component is basic parts such as door, window, seat and etc. The second component is the system such as wiper system, steering system, braking system and etc. Most of car makers spend a lot of money in research and development to reduce the unwanted noise and vibration happen in cars passenger (Shinya Goto et.al, 2001).

Noise and vibration in wiper system can divided into three categories that are squeal noise, chattering noise and reversal noise. Squeal noise also known as a squeaky noise, is a high frequency sound and range about 1000 Hz. The chattering noise also called as beep noise and it is a low frequency with the range of 100 Hz and less. Reversal noise is an impact sound of 500 Hz and less and it was generated when rubber inside the wiper bumps against the glass when the wiper reverses (Shinya Goto et.al., 2001), (Stalleart et.al., 2006), (Regis et.al., 2002), (A.R. Abu Bakar et.al., 2008).

Numerical and analytical study has been made to make the comparison between the prediction results and the numerical results. Hence, the correlation is reasonably close. The main objective to make verification test is to ensure the data more reliable and trustworthy before further analysis.

In these studies, an input shaping scheme (IS) has been applied to the wiper system in order to reduce the unwanted noise and vibration. Two impulse sequences input shaper is a technique in IS and it was implemented into this study. After applying the IS, the level of unwanted noise and vibration occurs in wiper system is slightly reduced.

The main goal of this study is to show the effectiveness of IS applied to the wiper system. By implementing the IS, it is found that the level of unwanted noise and vibration was reduced up to 30 percent compare without using IS.

2.0 WIPER ANALYTICAL MODEL

Figure 1 show the spring mass model of arm and blade for wiper system (Shigeki et.al., 2000), Table 1 shows the condition of blade rubber (Shigeki et.al., 2000).

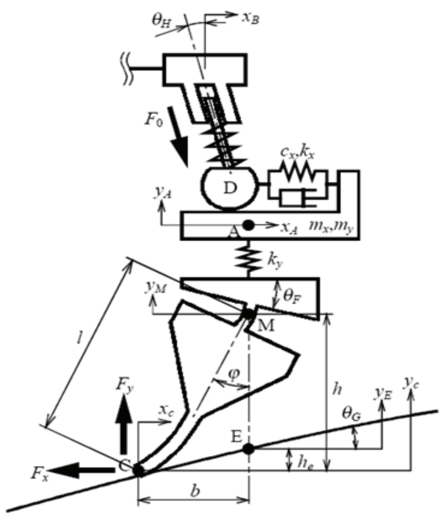

FIGURE 1
Spring mass model of arm and blade (Shigeki et.al., 2000)

TABLE 1
Condition of rubber blade (Shigeki et.al., 2000)

Condition	C	D	Variable
A			y_A, θ_a

Where:

A = No contacted condition between rubber shoulder and rubber head.
C = It is a stick condition between the blade lip on the windshield
D = It is a slipped condition

The parameters used in the analytical model are listed in Table 2. The subscripts in vector i represent the position of rubber claw and vector j represents the position along the rubber element. These two vectors were illustrated by Figure 1 and then representing in Figure 2.

TABLE 2
Parameters in analytical model

Parameter	Description
l_A	Arm length
l_B	Blade length
n_s	Number of claw position
n_z	Number of rubber decomposition
l_Z	Length of rubber element ($l_Z = l_B/n_z$)
d_{mj}	Distance from pivot to rubber element
m_x	Equivalent mass of arm and blade to the x-axis
m_y	Equivalent mass of arm and blade to the y-axis
m_{Ax}	Arm equivalent mass in the x-direction
m_{Ay}	Arm equivalent mass in the y-direction
m_B	Blade mass
m_R	Rubber mass
m_r	Rubber element mass ($m_r = m_R/n_z$)
c_x	Equivalent damping coefficient of arm to the x-axis
k_x	Equivalent spring constant of arm to the x-axis
x_B	Arm tip virtual position without arm deformation
y_m	Neck rotation center position
θ_H	Arm head twist angle
θ_F	Arm front twist angle
θ_G	Windshield grass profile
F_0	Arm pressure

Parameter	Description
l_A	Arm length
l_B	Blade length
n_s	Number of claw position
n_z	Number of rubber decomposition
l_Z	Length of rubber element ($l_Z = l_B/n_z$)
d_{mj}	Distance from pivot to rubber element
m_x	Equivalent mass of arm and blade to the x-axis
m_y	Equivalent mass of arm and blade to the y-axis
m_{Ax}	Arm equivalent mass in the x-direction
m_{Ay}	Arm equivalent mass in the y-direction
m_B	Blade mass
m_R	Rubber mass
m_r	Rubber element mass ($m_r = m_R/n_z$)
c_x	Equivalent damping coefficient of arm to the x-axis
k_x	Equivalent spring constant of arm to the x-axis
x_B	Arm tip virtual position without arm deformation
y_m	Neck rotation center position
θ_H	Arm head twist angle
θ_F	Arm front twist angle
θ_G	Windshield grass profile
F_0	Arm pressure

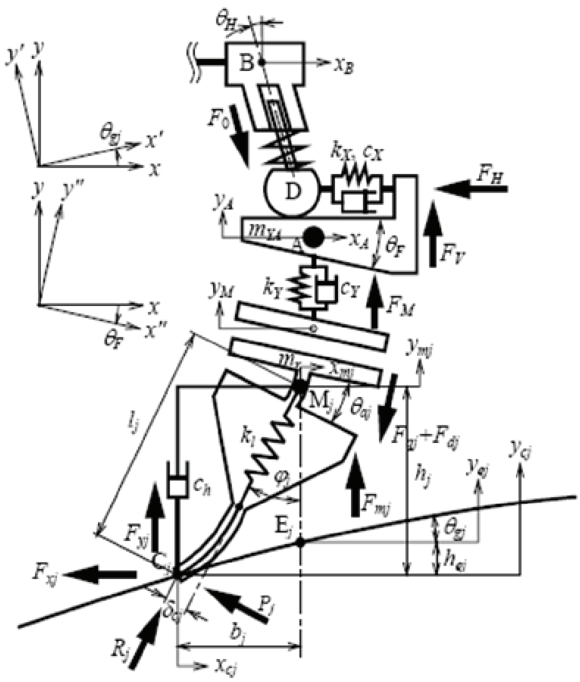

FIGURE 2
Vector position in arm and blade (Shigeki et.al., 2003)

In this study, the rubber blade at A and C condition was selected as an initial position of wiper blade. These initial conditions represent the contact condition between the rubber shoulder with the rubber head and the stick condition between the blade lips on the windshield. The vector position in this initial position is shown in Figure 2. Here, the vector function of wiper system is neglected (Shigeki et.al., 2003).

3.0 MATHEMATICAL MODEL OF WIPER SYSTEM

The derivation of mathematical model in A and C condition is focused on the forces at y-direction. Figure 1 shows the description of rubber blade and the location of rotating point at M_r and the length of the rubber given by l. Therefore,

$$l = \frac{l_a}{2} + l_b + l_c \tag{1}$$

The reaction force P can be generate by deforming of rubber as,

$$P = \frac{k_a \theta_a}{l} = k_c \delta_c \tag{2}$$

The relationship between the force P, force at x-direction F_x and the force at y-direction F_y is follow by,

$$F_x cos\varphi + F_y sin\varphi = P \tag{3}$$

Where

$$\varphi = \theta_a + \theta_F$$

By doing this derivation, the assumption for equation 3 are based on Figure 1 and the assumption are,

1. Arm is twisted as a rigid body motion
2. No friction effect except mass included
3. Not leave the horizontal plane of the top arm

By the assumption, the origin if at x-direction where these positions mark that the crank arm was set without any deformations for each spring. The setting at every initial position except the spring has a pressure F_0 and the spring of blade with constant condition k_y.

The origin point are located at y_A and y_M. Point of M is $\theta_A=\delta_c=0$ and $x_A=0$. The origin point of the y_C and y_E at point E at y-direction. Since the spring constant for F_0 is zero, the spring constant will replaces by constant parameter automatically. When the system is unbalanced, the origin with the parameter θ_H and θ_F can be defined as a initial position at t=0 and based on this condition, an equilibrium condition with $\theta_a=\delta_c=0$ can be made. These equilibrium condition has an initial reaction forces at F_{x0} and F_{y0}, and then can be derived as,

$$F_0 = F_{y0}cos\theta_H + F_{x0}sin\theta_H$$

$$= F_{x0}cos\theta_F + F_{y0}sin\theta_F$$

$$F_{y0}sin\theta_F = -F_{x0}cos\theta_F$$

$$F_0 = \frac{-F_{x0}cos\theta_F cos\theta_H}{sin\theta_F} + F_{x0}sin\theta_H$$

$$F_0 = \frac{F_{x0}(sin\theta_H sin\theta_F - cos\theta_F cos\theta_H)}{sin\theta_F}$$

$$F_{x0} = \frac{-sin\theta_F . F_0}{(cos\theta_F cos\theta_H - sin\theta_F sin\theta_H)} \tag{4}$$

The equation of reaction forces acring at x and y-direction can sumarize as,

$$F_{x0} = \frac{-sin\theta_F}{cos(\theta_H + \theta_F)} F_0 \tag{5}$$

$$F_{y0} = \frac{cos\theta_F}{cos(\theta_H + \theta_F)} F_0 \tag{6}$$

The value of $F_{x0} \neq 0$ when the value of $\theta_F \neq 0$ in equation 4. The sum of force in x-direction can be derived as,

$$m_x \ddot{x}_A + c_x(\dot{x}_A + \dot{y}_A tan\theta_H - \dot{x}_B) + k_x(x_A + y_A tan\theta_H - x_B) + F_{x0} = 0 \tag{7}$$

The sum of force in y-direction can be derived as,

$$m_y \ddot{y}_A + c_y(\dot{y}_A - \dot{y}_C) + \{c_x(\dot{x}_A + \dot{y}_A tan\theta_H - \dot{x}_B) + k_x(x_A + y_A tan\theta_H - x_B)\}tan\theta_H - F_{y0} = 0 \tag{8}$$

Where

$$F_y = -k_y(y_A - y_M) + F_{y0}$$

The equation of mathematical model for AC condition in x and y-direction can be simplified by using equation 5 and 7 for x-direction and 6 and 8 for y-direction, respectively. The new equation represent in equation 9 and 10 for both x and y-direction.

$$m_x(\ddot{x}_c + \ddot{b}) + c_x((\dot{x}_c + \dot{b}) + \dot{y}_A tan\theta_H - \dot{x}_B) + k_x((x_c + b) + y_A tan\theta_H - x_B) + F_{x0} = \frac{-sin\theta_F}{cos(\theta_H + \theta_F)} F_0 = 0 \tag{9}$$

$$
\begin{aligned}
m_y \ddot{y}_A + c_y\big[\dot{y}_A - \{(\theta_G - l\theta_G sin\varphi)\dot{x}_A - l\theta_G\dot{\theta}_a cos\varphi\}\big] \\
+ c_x\left\{\left(l\dot{\theta}_a\left\{\left(1+\frac{1}{K}\right)cos\varphi - \left(\frac{\theta_a}{K}\right)sin\varphi\right\}\right) + (\dot{y}_A tan\theta_H - \dot{x}_B)\right. \\
+ k_x\left\{\left(x_c + l\left\{sin\varphi + \left(\frac{\theta_a}{K}\right)cos\varphi\right\} + y_A tan\theta_H - x_B\right)\right\} tan\theta_H\Big\} \\
- \left[-k_y(y_A - y_M) + \frac{cos\theta_F}{cos(\theta_H - \theta_F)}F_o\right] + \frac{cos\theta_F}{cos(\theta_H - \theta_F)}F_o \\
= 0 \qquad (10)
\end{aligned}
$$

Equations 9 and 10 have been used in analytical approach to investigate the level of unwanted noise and vibration in wiper system. The result is a predicted result and requires validating by using the result in experimental approach before further analysis.

4.0 VERIFICATION OF THE MATHEMATICAL MODEL BETWEEN ANALYTICAL AND NUMERICAL APPROACH

In this study, there are factors to be considered by using analytical approach and they are development and verification of two dimensional mathematical models. This verification process is necessary to make the result more reliable and trustworthy before further analysis is made. Figure 3 and Figure 4 shows the result from analytical and numerical approach.

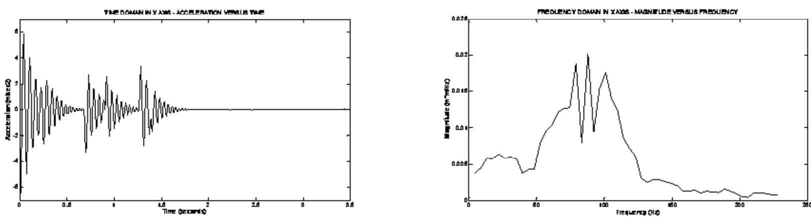

FIGURE 3
Analytical result for time and frequency domain in x-direction

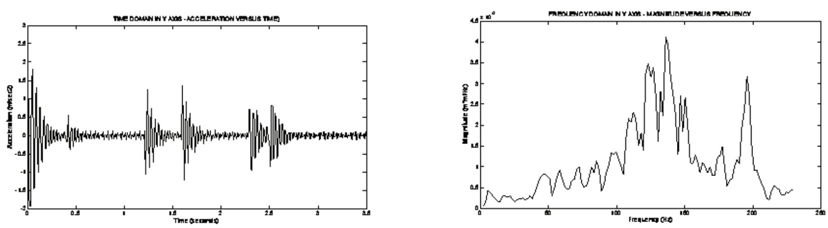

FIGURE 4
Analytical result for time and frequency domain in y-direction

In x-direction, the maximum level of unwanted noise and vibration are 4.3 m/sec2 and 0.02 m*m/Hz, respectively. The maximum level of unwanted vibration is located at 92.72 Hz. In y-direction, the level of unwanted noise and vibration are 1.5 m/sec2 and 4.2 x 10-3 m*m/Hz and located at 128.2 Hz. Numerical approach is one of the method that can be used to investigate the level of unwanted noise and vibration for wiper system (Ibrahim et.al., 2006). Thus, the result from this numerical approach can be used to verify the result in analytical approach. Figure 5 and Figure 6 show the result of numerical approach in x and y-direction.

In this verification process, the percentage of error for both x and y-direction are less than 7 percent and the result are shown in Figure 7 and Figure 8 for x and y-direction, respectively.

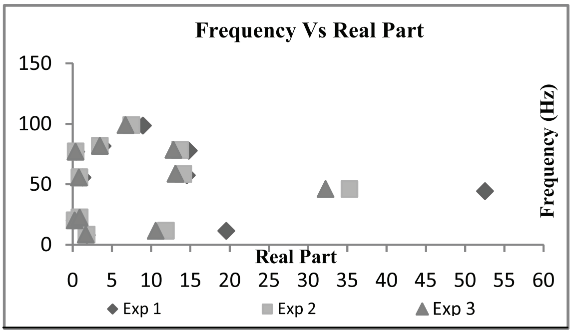

FIGURE 5
Numerical result in x-direction

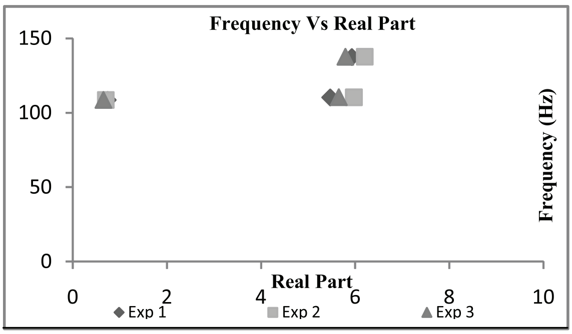

FIGURE 6
Numerical result in y-direction

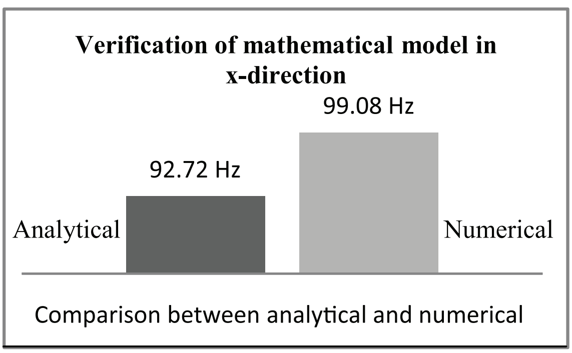

FIGURE 7
Verification result in x-direction

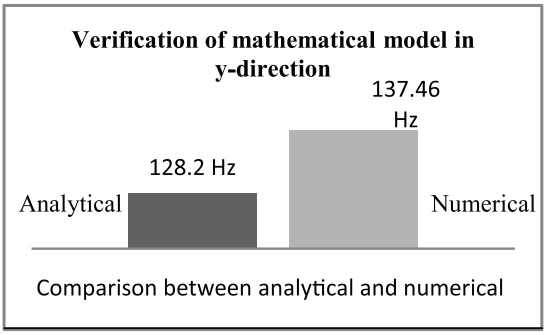

FIGURE 8
Verification result in y-direction

5.0 INPUT SHAPING SCHEME (IS)

Input shaping scheme (IS) involve convolving desired command by the sequencing of impulses. It also known as an input shaper where the system has a potential to create the shaped system commands. This IS has a good potential to eliminate or reduce the unwanted noise and vibration at certain amplitude, time location and frequency which depends on the characteristics of the system. The IS can made insensitive to make a variation in a resonant frequency (Chen et.al., 2007). It is also more effective to minimize vibration level especially in flexible system that the frequency shifts during moves such as wiper system has been used in this study. This section represents the details of the derivation of IS method and also an overview of implementation of IS.

The vibratory system of any order either in static, dynamics or flexible systems can be modeled as a superposition of second order system (M.Z.Md Zain et.al., 2002). The transfer function gives by,

$$G(s) = \frac{\omega_n^2}{s^2 + 2\xi\omega_n s + \omega_n^2} \tag{11}$$

Where

ω_n = natural frequency
ξ = damping ration of the system

Then, the impulse response of the system can be derived as a,

$$y(t) = \frac{A\omega_n}{\sqrt{1-\xi^2}} e^{-\xi\omega_n(t-t_o)} sin\left[\omega_n\sqrt{1-\xi^2(t-t_o)}\right] \tag{12}$$

Where

A = amplitude
t_o = time of the impulse

The response of the impulses can represent by the superposition of the impulse response. For N impulse with $\omega_d = \omega_n \sqrt{(1-\xi^2)}$.

The impulses can be expressed by,

$$y(t) = Msin(\omega_d t + \alpha) \tag{13}$$

Where

$$M = \sqrt{\left(\sum_{i=1}^{N} B_i cos\Phi_i\right)^2 + \left(\sum_{i=1}^{N} B_i cos\theta_i\right)^2} \tag{14}$$

$$B_i = \frac{A_i \omega_n}{\sqrt{1-\xi^2}} e^{-\xi\omega(t-t_i)} \tag{15}$$

$$\Phi_i = \omega_d t_i \tag{16}$$

$$\alpha = tan^{-1}\left(\sum_{i=1}^{N} \frac{B_i cos\Phi_i}{B_i sin\Phi_i}\right) \tag{17}$$

Where

A_i = magnitudes
t_i = times

These can be occurred by the impulses response. The residual single mode amplitude of the vibration and it is according on the repulse response and it can be evaluated at the time of the last impulse happen, t_N. It can be expressed by,

$$V = \sqrt{V_1^2 + V_2^2} \tag{18}$$

Where

$$V_1 = \sum_{i=1}^{N} \frac{A_i \omega_n}{\sqrt{1-\xi^2}} e^{-\xi\omega_n(t_N-t_i)cos(\omega_d t_i)} \tag{19}$$

$$V_2 = \sum_{i=1}^{N} \frac{A_i \omega_n}{\sqrt{1-\xi^2}} e^{-\xi\omega_n(t_N-t_i)sin(\omega_d t_i)} \tag{20}$$

To achieve the zero vibration after the input has ended, it is required that both V_1 and V_2 are directly equal to zero. The shaped command input has gives the same values of rigid body motion likely as an unshaped command and it is required to make a summation of the amplitude of impulses is unity. To avoid this delay time, the first impulses is set to zero base on time. So, the value of V_1 and V_2 are required to be zero.

Thus,

$$\sum_{i=1}^{N} A_i = 1 \tag{21}$$

It is required to solve using a yield of four impulse response sequence with parameters in equation 22 to 24.

$$t_1 = 0, t_2 = \frac{\pi}{\omega_d}, t_3 = \frac{2\pi}{\omega_d}, t_4 = \frac{3\pi}{\omega_d} \tag{22}$$

$$A_1 = \frac{1}{1 + 3K + 3K^2 + K^3}, A_2 = \frac{3K}{1 + 3K + 3K^2 + K^3} \tag{23}$$

$$A_3 = \frac{3K^2}{1 + 3K + 3K^2 + K^3}, A_4 = \frac{K^3}{1 + 3K + 3K^2 + K^3} \tag{24}$$

Where

$$K = e^{\frac{-\xi\pi}{\sqrt{1-\xi^2}}} \tag{25}$$

The higher vibration responses in this scheme are handled when an impulse sequence for each vibration mode is designed independently. An impulse is convolved jointly with higher mode.

6.0 ANALYSIS AND DISCUSSION

The simulation results using IS are shown in Figure 9 and Figure 10 in time and frequency domain by x- and y-direction, respectively. Using IS, the result indicates that this scheme has given a good improvement to reduce the level of unwanted noise and vibration in wiper system.

The level of unwanted noise and vibration by implementing IS for x- and y-direction are 3.7 m/sec2 and 0.015 m*m/Hz for x-direction, 1.3m/sec2 and 2.7 x 10-3 m*m/Hz for y-direction. Based on this result, IS has a potential to reduce the unwanted noise and vibration generated by wiper system.

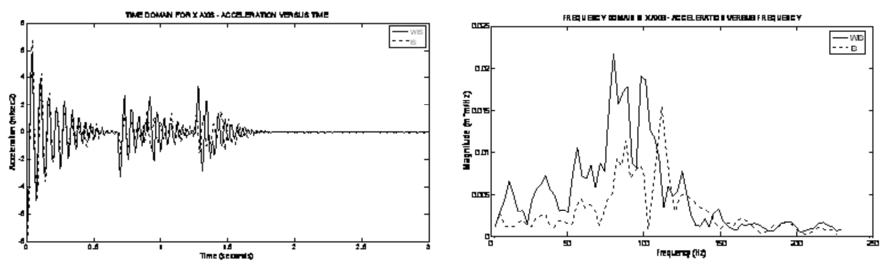

FIGURE 9
IS for time and frequency domain in x-direction

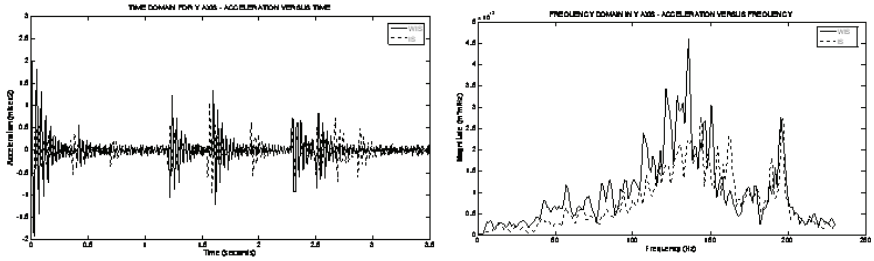

FIGURE 10
IS for time and frequency domain in y-direction

7.0 CONCLUSION

Comparison between analytical and numerical approach concluded that the correlation is reasonably closed. In this correlation, the result in analytical approach can use for further analysis. To reduce the level of unwanted noise and vibration in wiper system, input shaping scheme (IS) has implemented to two dimensional mathematical models of wiper system. There are good agreement to reduce the noise and vibration.

8.0 ACKNOWLEDGEMENT

The author would like to thank to the Malaysian Ministry of Higher Education (MOHE) under Vot No.78190 and also thank to the Research Management Center, Universiti Teknologi Malaysia and Universiti Teknikal Malaysia Melaka.

9.0 REFERENCES

A.R. Abu Bakar, M.Z. Md Zain. 2008. Modeling and Simulation Wiper Noise and Vibration using Finite Element Method. 2nd Regional on Vehicle Engineering and Technology 2008.

B.Stalleart, F.Daucet, J.Rys. 2006. Application of Dither Control for Automotive Wiper Squeal. Proceeding of ISMA2006.

Chen Yang Lan, Suhada Jayasuriya. 2007. Why Use Input Shaping and Not Feedback Control. 8th International Symposium on Quantitative Feedback Theory and Robust Frequency Domain Methods.

Ibrahim Marzukie, Abd Rahim Abu Bakar. 2006. Modeling and Simulation of an Automotive Wiper Noise and Vibration using Finite Element Method. ICAME09. Accepted.

M.Z.Md, G.Priyandoko, M.Mailah. 2002. Performance of Hybrid Control Scheme AFC and Input Shaping For A Suspension System. Project Report. Faculty of Mechanical Universiti Teknologi Malaysia, Malaysia.

Regis Grenouillat, Christian Leblanc. 2002. Simulation of Chatter Vibrations for Wiper

System. SAE Technical Paper Series. 2002-01-1239.

Shigeki Okura, Takio Oya. 2003. Complete 3D Dynamics Analysis of Blade Reversal Behavior in a Windshield Wiper System. SAE Technical Paper Series. 2003-01-1373.

Shigeki Okura, Tohru Sekiguchi, Takio Oya. 2000. Dynamics Analysis of Blade Reversal Behavior in a Windshield Wiper System. The Engineering Society for Advancing Mobility Land Sea Air and Space (SAE). 2000-01-0127.

Shinya Goto, Hiroshi Takahashi, Takio Oya. 2001. Clarification of the Mechanism of Wiper Blade Rubber Squeal Noise Generation. JSAE Review 22 (2001) 57-62.

Shinya Goto, Hiroshi Takahashi, Takio Oya. 2001. Investigation of Wiper Blade Squeal Noise Reduction Measures. Society of Automotive Engineers. 2001-01-1410.